Research Article

Protective Effects of Ginger Ethanolic Extract, Chitosan Nanoparticles, and Ginger Ethanolic Extract-Loaded Chitosan Nanoparticles on Pancreatic DNA Damage and Histological Changes in Dogs with Alloxan-Nicotinamide Induced Type 2 Diabetes

Rasema Majeed, Alaa Kamil Mahmood*

Department of Veterinary Internal and Preventive Medicine, College of Veterinary Medicine, University of Baghdad, Baghdad, Iraq.

Abstract | Type 2 diabetes (T2D) is associated with increased oxidative stress and DNA damage. Natural products such as ginger ethanolic extract (GEE) have antioxidant and anti-inflammatory properties that may help in mitigate these effects. Chitosan nanoparticles (CNPs) can improve delivery and bioavailability of encapsulated agents such as GEE. The aims of this study to evaluate the protective effects of ginger ethanolic extract, chitosan nanoparticles, and ginger ethanolic extract loaded with chitosan nanoparticles (GEE-CNPs) against DNA damage and pancreatic histological changes in dogs with alloxan-nicotinamide-induced diabetes. histological analysis was assessed. The results showed that first group (Control negative) administered distilled water showed no abnormal lesion, while second group (Control positive) is diabetic without treatment showed destruction and necrosis of islet cells, congestion and edema between their acini. Third group was administered 81.7 mg/kg BW of ginger ethanolic extract orally for 45 days showed normal section of islet cells shows moderate necrosis and destructions of islet cells. congested blood vessels, regeneration of islet cells. fourth group was administered 81.7 mg/kg BW of ginger ethanolic extract loaded with chitosan nanoparticles orally for 45 days and showed normal section of islet cells, regeneration of islet cells also showed no clear lesions in the islet cells. whereas fifth group was administered 81.7 mg/kg of chitosan nanoparticles orally for 45 days and showed few destructions and vacuolation in the islet cells, regeneration of the islet cells. Pancreatic DNA damage analysis were assessed the results showed that ginger ethanolic extract, chitosan nanoparticles, and ginger ethanolic extract loaded with Chitosan nanoparticles all significantly reduced DNA damage compared to saline From this study concluded ginger ethanolic extract loaded with chitosan nanoparticles provided greater protection than ginger ethanolic extract or chitosan nanoparticles alone. Encapsulation of ginger ethanolic extract in chitosan nanoparticles enhances these protective effects, warranting further research into ginger ethanolic extract loaded with Chitosan nanoparticles as a therapeutic agent for diabetes.

Keywords | *Zingiber officinale*, Chitosan, Nanoparticles, Ethanolic extract, Type 2 diabetes, Dog, Herbal medicine, Oxidative stress, Histopathology

Received | October 16, 2023; **Accepted** | October 27, 2023; **Published** | December 15, 2023
***Correspondence** | Alaa Kamil Mahmood, Department of Veterinary Internal and Preventive Medicine, College of Veterinary Medicine, University of Baghdad, Baghdad, Iraq; **Email:** alaa.k@covm.uobaghdad.edu.iq
Citation | Majeed R, Mahmood AK (2024). Protective effects of ginger ethanolic extract, chitosan nanoparticles, and ginger ethanolic extract-loaded chitosan nanoparticles on pancreatic DNA damage and histological changes in dogs with alloxan-nicotinamide induced type 2 diabetes. Adv. Anim. Vet. Sci., 12(1): 32-43.
DOI | http://dx.doi.org/10.17582/journal.aavs/2024/12.1.32.43
ISSN (Online) | 2307-8316

INTRODUCTION

Diabetes mellitus is a chronic metabolic disorder that poses a significant health burden for both humans and animals, including dogs (O'Kell and Davison, 2023). Characterized by persistently elevated levels of blood glucose (hyperglycemia), the disease often results from inadequate insulin production or ineffective insulin utilization (Nelson and Reusch, 2014). In the canine population, the requirement for exogenous insulin is pivotal to maintain glycemic control and to prevent severe complications such as ketoacidosis (Niessen et al., 2022).

Persistent hyperglycemia in diabetes mellitus has been associated with elevated levels of reactive oxygen species (ROS) and oxidative stress (Papachristoforou et al., 2020). The detrimental impact extends to cellular damage and complications in various organ systems (Davison, 2018). Specifically, DNA damage is a concerning consequence that has been observed in both human and animal models of Type 2 Diabetes (T2D) (Akash et al., 2015). Additionally, histological changes, such as damage to pancreatic beta cells and disorganized islet cell architecture, are commonly reported (Poitout and Robertson, 2008). Histopathological descriptions of pancreases affected dogs reflect a various process, including degenerative changes in pancreatic islets with vacuolation, lymphocytic infiltration and generalized pancreatic inflammation have also been reported (O'Kell et al., 2017).

Traditional medicine has long used ginger (*Zingiber officinale*) as a commonly used medicinal plant (Garza-Cadena et al., 2023). This Zingiberaceae family member originates from Southeast Asia, different biologically active substances, including gingerols, shogaols, paradols, and zingerone, give ginger its distinct flavor and aroma (Zhang et al., 2021). These compounds have been found to have anti-inflammatory, antimicrobial, anticancer, antidiabetic, and antioxidant properties (Al-Salman et al., 2022; Ameer and Al-Deen, 2023).

Ginger (*Zingiber officinale*) has gained scientific attention for its potential therapeutic benefits in diabetes mellitus (Akash et al., 2013; Mustafa, 2023). A variety of studies have reported improvements in glycemic control, lipid profiles, and inflammatory markers in both human patients and animal models of T2D (Abdulrazaq et al., 2012; Arablou et al., 2014). Ginger has also shown protective effects against diabetic complications in multiple organs (Li et al., 2012).

Chitosan nanoparticles (CNPs) are emerging as a novel therapeutic approach for diabetes mellitus (Priyanka et al., 2022). Chitosan's wide range of bioactivities includes protecting pancreatic beta cells, lowering hyperglycemia, preventing impaired lipid metabolism, immunomodulating, and stimulating the enhancement of wound healing (Mahmood and Alwan, 2015; Salih et al., 2015). Moreover, CNPs have been studied for their potential as a drug delivery system, demonstrating biocompatibility and sustained release properties (Mohammed et al., 2017; Nie et al., 2020; Jasim, 2021).

To the best of our knowledge, there is a clear lack of studies examining the effects of ginger and CNPs on dogs with T2D, although promising therapeutic properties of both. Due to ginger's anti-inflammatory, antioxidant, and antidiabetic bioactive components like gingerols and shogaols, as well as the drug delivery advantages of CNPs, there is a need for more research into this area (Mahmood and Alwan, 2019; Sanjib et al., 2020). Therefore, this study aims to fill this research gap by investigating the therapeutic potential of ginger ethanolic extract (GEE), CNPs, and GEE-loaded CNPs on pancreatic DNA damage protection and histological changes in a canine model of T2D induced by alloxan-nicotinamide combination.

MATERIALS AND METHODS

Plant materials and extraction

Zingiber officinale rhizomes were obtained from a local market in Baghdad province, Iraq and formally authenticated by the Iraqi National Herbarium, Directorate of Seed Testing and Certification belong to the Iraqi Ministry of Agriculture with a certified No. of 2860 in April 2022.

The ginger rhizomes were chipped, air-dried, and ground by an electrical blender into a fine powder. Then, amount of 50 g of the powder was soaked in 200 mL of ethanol (70%, Alpha Chemika, Indea) and left over night in a conical flask at room temperature. Afterward, the mixture was filtered by a fine muslin cloth to remove solid particles. The filtration residue was then extracted again twice using the same procedure, and the resulting mixture was filtered through Whatman filter paper No. 1 to obtain a clear extract. The mixture was concentrated by a vacuum rotary evaporator (Heidolph, Germany) at 40 °C. Finally, the concentrated extract was placed in an oven at a temperature of 45 °C until the solvent was evaporated. The resulting extract was stored in a clean container until it was used for phytochemical analyses (Nikolić et al., 2014).

Synthesis of chitosan nanoparticles and ginger ethanolic extract-loaded chitosan nanparticles

Four different concentrations were prepared from a chitosan (Avonchem Ltd, UK, 9999% purity, CAS: 9002-4, Batch No: AC00671K, 100MPa.s) solution,

following the modulating method of (Pires et al., 2014) Concentrations of 0.25, 0.5, 1, and 2 mg/mL of chitosan solution were prepared by adding 25, 50, 100, and 200 mg of chitosan powder to 100 mL of deionized distilled water (dDW) containing acetic acid (CDH, India) at 1% v/v. The mixture was soaked for 24 hours at room temperature. Then, continuous stirring was performed using a magnetic bar in a hotplate stirrer at 900 rpm for 30 minutes, resulting in the formation of a semi-colloidal solution. A pH meter (Hanna Instruments SRL, Romania) was used to determine the need for NaOH (0.1 N, CDH, India) to bring the pH down to 4.6, and then the solution was sonicated for 3 minutes in a probe sonicator (Misonix Inc, Germany). Filter paper (Whitman No. 1) was then used to filtrate the solution

The loading of ginger extract on CNPs was carried out using an ionic gelation method, following the procedures described by Ibrahim et al. (2015) and Ali et al. (2018) with some modifications. Initially, 200 mg of ginger extract was dissolved in 1 mL of propylene glycol and added dropwise to 100 mL of chitosan solution (2 mg/mL) at a 1:1 loading ratio of ginger extract to chitosan. The mixture was continuously stirred on a hot plate stirrer for 30 minutes at 900 rpm. Subsequently, the solution was sonicated for 1 minute, returned to continuous stirring, and 20 mL of sodium tripolyphosphate solution (TPP, Daejung, Korea) at 0.25% w/v was added dropwise at a ratio of 5:1. The mixture was stirred for an additional 30 minutes to allow ginger extract particles to adsorb onto the surface of the chitosan particles. The solution was then sonicated (Misonix Inc., Germany) for 1 minute and filtered using filter paper Whitman No. 1 to remove non-bound particles. The solution was centrifuged at 10000 rpm for 15 minutes, after the supernatant was discarded, the sedimented pellets were washed with distilled water, collected, and freeze-dried for 24 hours and kept at 4 °C for subsequent use. This resulted in ginger extract loaded on chitosan nanoparticles.

Physicochemical characterization

Fourier transform infrared spectroscopy (FTIR)

Analysis of chemical bonding and functional groups was performed using TENSOR 27 (German)FTIR spectrophotometerThe solutions underwent centrifugation at 10000 rpm for 15 minutes, followed by three washes with dDW to remove any unconnected particles. The samples were then dried at 40 °C and mixed with a pure binder potassium bromide (KBr) and placed inside discs under high pressure. The FTIR analysis was conducted within the wavelength range of 400-4000 cm^{1}, where the spectroscopy exhibited peaks representing the transmittance range of infrared rays at specific frequencies corresponding to the functional groups of each material (Abo Mansour et al., 2020; Al-Saadi, 2020).

Atomic force microscopy (AFM)

The surface morphology and size of the nanoparticles were analyzed using Angstrom AA2000 AFM, contact mode, atmospheric conditions at the Department of Chemistry, College of Science, Al-Nahrain University, Baghdad, Iraq. The obtained AFM images were analyzed to determine the size distribution, surface roughness, and topographical features of the nanoparticles. AFM images were analyzed using image processing software to extract information on size distribution, surface roughness, and topographical features of the nanoparticles (Jabar, 2020).

Ethical approval and animals

This research involving animals was carried out in accordance with the ethical guidelines provided by the local Animal Care and Use Committee at the College of Veterinary Medicine, University of Baghdad. The study was reviewed and approved by the Research Ethics Committee (Protocol Number: 549/P.G. dated 8 May 2023), ensuring that all procedures performed in this study were in line with ethical standards.

Experimental design

Twenty clinically healthy local breed mongrel dogs of both sexes, with ages ranging from 7 to 13 months and body weights within a range of 11-19 kg, obtained from a commercial supplier in Baghdad province were included in the study. All experimental animals were clinically examined and housed in the animal house belongs to the Department of Surgery and Obstetrics, College of Veterinary Medicine, University of Baghdad, where they experienced controlled environmental conditions characterized by moderate temperature and a 12-hour light and 12-hour dark cycle. As a part of the acclimatization process, the animals were housed in cages (1×2×1 m^{3}) for a duration of two weeks prior to the commencement of the experiment, in which they were provided with standard dog food consisting of standard pellets, meat, and bread, offered twice daily (morning and evening), and had constant access to tap water throughout the experimental period.

The dogs were randomly allocated into one of five groups. The group 1 (Negative Control) served as a non-diabetic control, showing the baseline conditions without diabetes induction, while the remaining sixteen dogs were designated for experimental induction of T2D. Prior to the induction process, all dogs were fasted for a period of 18 hours. According to Bruyette (2013), the established normal range for blood glucose levels in healthy dogs is between 75 and 120 mg/dL, and the renal glucose threshold is approximately 180 mg/dL. T2D was experimentally induced using a modified protocol

proposed by Areej and Abbas (2019), originally adapted from Vattam et al. (2016) and further elaborated by Sari et al. (2020). Each dog received an intravenous single injection of alloxan (Ax) monohydrate (CDH, India, 70 mg/kg BW) and nicotinamide (Nm) (Avonchem, UK, 50 mg/kg BW), dissolved in a 0.9% sodium chloride solution. Nicotinamide was administered 30 minutes prior to the injection of alloxan to partially protect pancreatic beta (β)-cells from alloxan-induced toxicity (Uchigata et al., 1983). Blood glucose levels were checked 72 hours post-induction using a glucometer (ACCU-CHEK, China). Dogs with blood glucose levels of higher than 140 mg/dL were considered diabetic.

Following diabetes induction, diabetic dogs (n=16) were further randomly subdivided into four treatment groups. Group 2 served as a positive control and received saline treatment; Group 3 was administered ginger ethanolic extract (GEE) at a dosage of 81.7 mg/kg BW; Group 4 was treated with GEE loaded-CNPs (GEE-CNPs), also at 81.7 mg/kg BW; and Group 5 received CNPs at the same dosage. All treatments were administered orally once daily for 6 weeks.

Histological examination

At the end of the study, one dog from each group was anesthetized and scarified using overdoes anesthesia (2% xylazine, VMD, Belgium, and ketamine (Alfasan, Holland)). Pancreatic tissue samples were collected and preserved in 10% buffered formalin for 48 hours for fixation. Tissue sections of 0.5 cm thickness were prepared and placed in plastic cassettes. These were then subjected to dehydration using an automated tissue processor (Histo-Line ATP700, Italy). Following this, the dehydrated tissues were embedded in paraffin using the HESTION TEC2800-C tissue embedding system (China). The paraffin-embedded tissues were subsequently trimmed and sectioned into 4-5 µm slices using a semi-automatic microtome (Histo-Line MRS3500, Italy). These sections were carefully placed in a water bath (FALC BI, Italy) and mounted on glass slides using a hot plate (Hysh11, Korea). Staining was performed using Hematoxylin and Eosin (H&E, Dakocytomation, Denmark), and the prepared slides were analyzed under a light microscope (Olympus, Japan) at 40x and 10x magnifications (Suvarna et al., 2018).

Comet assay for DNA damage assessment in pancreatic tissue

To evaluate DNA damage, the alkaline Comet Assay was performed according to Singh et al. (1988). Harvested pancreatic tissues were minced and homogenized, and the cells were isolated and suspended in Phosphate-Buffered Saline (PBS, Ca^{++}, Mg^{++} free, pH 7.4, HiMedia, Cat. No. TS1006) to a concentration of 10^5 cells/mL. Glass slides were precoated with 1% normal melting point agarose (HiMedia, Cat. No. RM273) and air-dried for substrate preparation. For the assay, a 100 µL aliquot of the cell suspension was mixed with 100 µL of 1% low melting point agarose (Sigma-Aldrich, Cat. No. A9414) at 37 °C. Immediately, this mixture was pipetted onto the precoated slides, which were then covered with coverslips. The slides were placed at 4 °C for 10 minutes to allow the agarose to gel. After gel formation, the coverslips were gently removed, and the slides were submerged in lysis buffer (containing 2.5 M NaCl, 100 mM EDTA, 10 mM Tris, and 1% Triton X-100, pH 10) and incubated overnight at 4 °C. The slides were then transferred to an alkaline unwinding solution (300 mM NaOH and 1 mM EDTA, pH >13) and incubated for 30 minutes at room temperature in the dark. Electrophoresis was conducted at 24 V (0.74 V/cm) and 300 mA for 30 minutes. Post-electrophoresis, 0.4 M Tris (pH 7.5) was used for 15 minutes to neutralize the slides. The DNA was stained with 100 µL of 10 µg/mL ethidium bromide (Sigma-Aldrich, Cat. No. E-8751). Comet images were captured using an Olympus BX53 fluorescence microscope at 40× magnification. DNA damage was quantified using Komet 5 image analysis software (Kinetic Imaging, Ltd., UK). The parameters measured included tail length, tail moment, and the percentage of DNA in the tail. A minimum of 50 to 100 randomly selected cells were analyzed per sample. Based on the calculated parameters, cells were scored from 0 (no tail) to 4 (almost all DNA in the tail) according to Collins et al. (2008), and categorized into four classes: Normal, cells with minimal or no tail length and low percent DNA in the tail; low damage, cells exhibiting moderate tail length and percent DNA in the tail; medium damage, cells with significant tail length and higher percent DNA in the tail; high damage, cells showing very high tail length and percent DNA in the tail.

Statistical analysis

Statistical analysis was performed using the computer program SPSS (version 16, 2007). The pancreatic DNA damage data were subjected to a one-way analysis of variance (ANOVA) followed by the least significant difference (LSD) post-hoc test to separate significant means at $P \leq 0.05$.

RESULTS AND DISCUSSION

Characterization

FTIR

The FTIR spectra of CNPs, GEE, and GEE-CNPs are shown in Figure 1A-C. The observed wavenumbers and corresponding functional groups of chitosan nanoparticles, ginger ethanolic extract, and ginger ethanolic extract-loaded chitosan nanoparticles are summarized in Tables 1, 2 and 3, respectively. The CNPs FTIR spectrum showed

characteristic peaks of the functional groups of chitosan, including hydroxyl (OH), amine (NH), alkane (CH), amide (C=O), ether (C-O), and amide (C-N) (Table 1). The GEE FTIR spectrum exhibited characteristic peaks associated with hydroxyl (OH), alkane (CH), carbonyl (C=O), and ether (C-O) functional groups (Table 2). Notably, the FTIR spectrum of GEE-CNPs demonstrated the presence of hydroxyl (OH), amine (NH), alkane (CH), amide (C=O), ether (C-O), and amide (C-N) functional groups (Table 3). This spectrum is a combination of the spectra from CNPs and GEE, showing that the ginger ethanolic extract was successfully loaded into the CNPs.

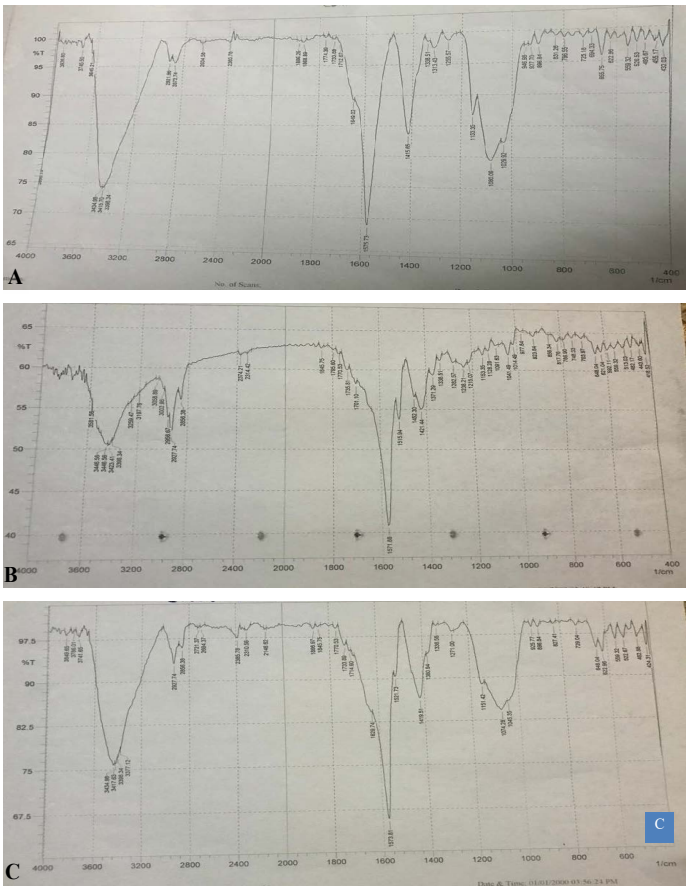

Figure 1: FTIR spectra of chitosan nanoparticles (A), ginger ethanolic extract (B), and ginger ethanolic extract-loaded chitosan nanoparticles (C).

Table 1: Wavenumbers (cm^{-1}) and corresponding functional groups as identified in the FTIR spectra of CNPs.

Wavenumbers (cm-1)	Functional group	Molecular vibration
3926.8, 3745.5, 3645.21	OH (hydroxyl)	O-H stretching
3434.98, 3415.7, 3398.34	NH (amine)	N-H stretching
2921.96, 2873.74	CH (alkane)	C-H stretching
1774.39, 1733.89, 1712.67, 1649.02	-C=O (amide)	C=O stretching
1575.73, 1415.65	CH (alkane)	C-H bending
1338.51, 1313.43, 1255.57	C-O (ether)	C-O stretching
1153.35, 1080.06, 1029.92	C-N (amide)	C-N stretching

Table 2: Wavenumbers (cm^{-1}) and corresponding functional groups identified in the FTIR spectra of GEE.

Wavenumbers (cm-1)	Functional group	Molecular vibration
3581.56, 3446.56, 3423.41, 3395.34, 3259.47	OH (hydroxyl)	O-H stretching
3197.76, 3058.89, 3002.96, 2956.67, 2927.74, 2856.38	CH (alkane)	C-H stretching
1795.6, 1770.53, 1735.81, 1701.	C=O (carbonyl)	C=O stretching
1571.88, 1515.94, 1452.3, 1421.44	CH (alkane)	C-H bending
1371.29, 1338.51, 1282.57, 1238.21, 1215.07	C-O (ether)	C-O stretching

Table 3: Wavenumbers (cm^{-1}) and corresponding functional groups identified in the FTIR spectra of GEE-CNPs.

Wavenumbers (cm-1)	Functional group	Molecular vibration
3849.65, 3786.01, 3741.65	OH (hydroxyl)	O-H stretching
3434.98, 3417.63, 3398.34, 3377.12	NH (amine)	N-H stretching
2927.74, 2856.38	CH (alkane)	C-H stretching
1795.6, 1774.39, 1733.89, 1712.67, 1649.02	C=O (amide)	C=O stretching
1575.73, 1515.94, 1452.3, 1421.44	CH (alkane)	C-H bending
1371.29, 1338.51, 1313.43, 1282.57, 1255.57	C-O (ether)	C-O stretching
1153.35, 1128.28, 1080.06, 1041.49, 1029.92	C-N (amide)	C-N stretching

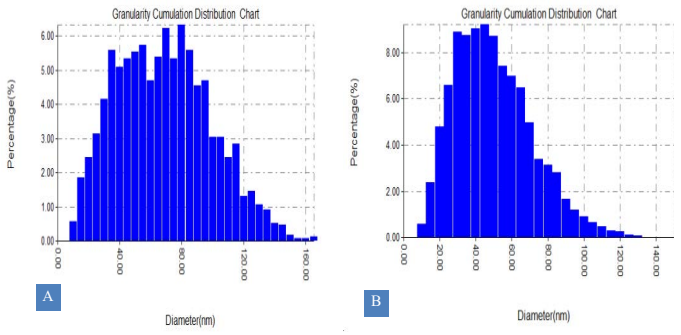

Figure 2: Average size of chitosan nanoparticles (CNPs) (A) and ginger ethanolic extract-loaded CNPs (GEE-CNPs) as obtained by atomic force microscopy.

AFM

The AFM analysis provided insights into the surface morphology, size distribution, surface roughness, and topographical features of the nanoparticles. The CNPs exhibited a uniform and spherical shape with an average size of 47.79 nm before loading (Figure 2A) and 66.31 nm after loading (Figure 2B). The increase in particle size

after loading can be attributed to the adsorption of ginger extract onto the surface of CNPs. The size and morphology of nanoparticles are important factors that influence their stability, bioavailability, and cellular uptake.

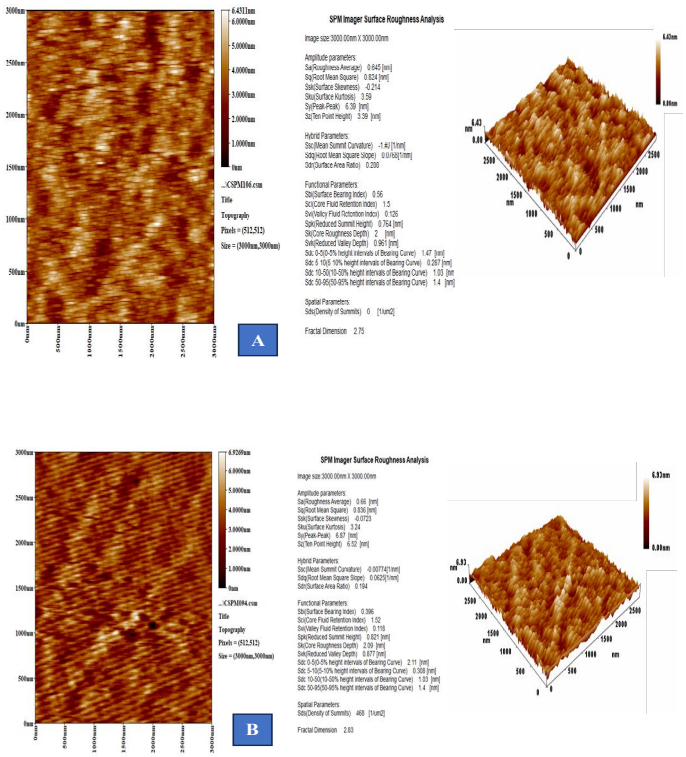

Figure 3: Atomic force microscopy of chitosan nanoparticles (CNPs) (A) and ginger ethanolic extract-loaded CNPs (GEE-CNPs) (B) synthesized using ionic gelation methods illustrate 2D and 3D topological.

In terms of surface roughness, the nanoparticles exhibited a roughness average (Sa) of 0.645 nm for CNPs and 0.66 nm for GEE-CNPs (Figure 3A, B). The root mean square (Sq) values were 0.824 nm and 0.836 nm, respectively. The topographical features of the nanoparticles showed variations in parameters such as surface skewness (Ssk), surface kurtosis (Sku), and peak-to-peak height (Sy). The Ssk values changed from -0.214 for chitosan nanoparticles to -0.0723 for ginger ethanolic extract loaded chitosan nanoparticles, indicating a more symmetric distribution of peaks and valleys on the surface after loading the extract. Sku values decreased from 3.59 to 3.24, suggesting a more uniform distribution of surface heights after loading the extract. Sy values showed minor changes, indicating that the overall height distribution remained similar after loading the extract.

Histological changes

The induction model of T2D was successfully established in dogs using alloxan and nicotinamide, as evidenced by the adverse histopathological changes in the positive control group (Group 2) compared to the Control Negative group (Group 1). Pancreatic tissue in the control group (non-diabetic, untreated) showed normal histological architecture with a well-organized exocrine component, consisting of acinar and ductal tissues, and an intact endocrine component, specifically the islets of Langerhans (Figure 4A, insertion). Group 2 (diabetic induced Ax-Nm, saline-treated), however, displayed significant pathological alterations, including inflammatory cells surrounding the acinar and ductal tissues and degeneration of the islets of Langerhans, with only one or two cells appearing normal (Figure 4B, insertion). In GEE-treated group (diabetic induced Ax-Nm, GEE-treated), exocrine tissue was morphologically normal and there was an improvement in the endocrine portion as evidenced with the presence of a few numbers of Langerhans cells (Figure 4C). However, Group 4, subjected to GEE-CNPs, demonstrated noticeable histological restoration. Both the exocrine component and the islets of Langerhans showed positive changes, with an activation and proliferation of cells in the latter suggesting an improvement in endocrine function (Figure 4D, insertion). Group 5, administered with CNPs alone, showed a histological pattern similar to Groups 3 and 4. Although there was an activation and proliferation of cells in the islets of Langerhans, indicating some level of endocrine improvement, the extent was notably less than what was observed in Group 4 (Figure 4E).

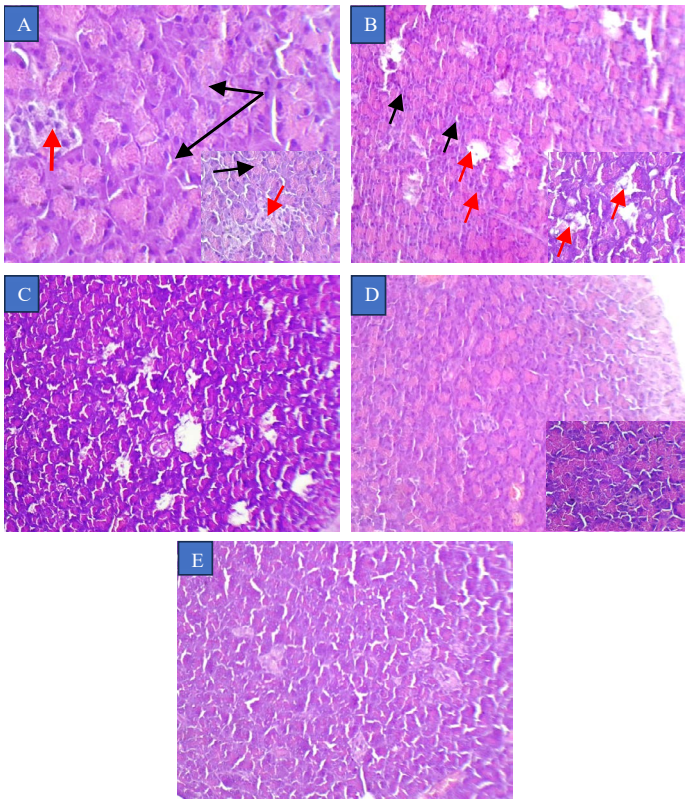

Figure 4: Pancrease in adult dog (H&E stain) in (A) Negative control group (non diabetic, not treated) showing normal tissue. (B) Positive control group (diabetic, saline treated) induced by alloxan–nicotinamide showing pancreatic damage. (C) Ginger ethanolic extract (GEE) group (diabetic, treated with 81.7 mg/kg BW GEE for 6 weeks) showing. (D) GEE-chitosan nanoparticles (GEE-CNPs) group (diabetic, treated with 81.7 mg/kg BW

GEE-CNPs) for 6 weeks) group showing. (E) CNPs group (diabetic, treated with 81.7 mg/kg BW CNPs) showing.

The histological findings affirm the efficacy of the T2D induction model and offer valuable insights into the therapeutic potential of GEE and CNPs. While treatment with GEE alone did yield a slight significant improvement, the formulation loaded with CNPs demonstrated promising results, especially in the regeneration of islet cells. Thus, it suggests a potential avenue for future research in the management of T2D in dogs.

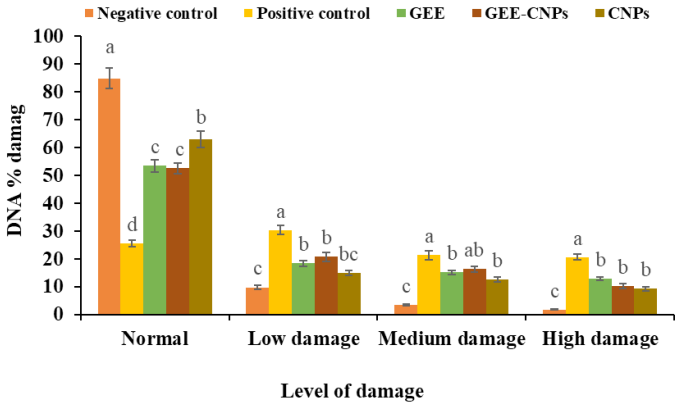

Figure 5: Comparative analysis of DNA damage categories in pancreatic tissue of dogs across different treatment groups. Negative Control group (non-diabetic, untreated), Positive Control group (diabetic, saline treated) induced by alloxan–nicotinamide). Ginger ethanolic extract (GEE) group (diabetic, treated with 81.7 mg/kg BW GEE for 6 weeks). GEE-chitosan nanoparticles (GEE-CNPs) group(diabetic, treated with 81.7 mg/kg BW GEE-CNPs for 6 weeks). CNPs group (diabetic, treated with 81.7 mg/kg BW CNPs for 6 weeks). Bars with different letters are statistically significant($P<0.05$). Error bars represent the standard error of mean(SEM).

Pancreatic DNA damage

The results of DNA damage evaluated across five groups: Negative Control, Positive Control, GEE, GEE-CNPs, and CNPs are presented in Figures 5 and 6. The percentage of cells with normal DNA and the levels of DNA damage were analyzed for each group to assess their respective protective effects against DNA damage. As expected for a negative control group, minimal DNA damage was observed. The cells in this group primarily fell into the normal category, constituting 84.86±3.67%. The range of DNA damage was minimum, spanning from 1.82±0.15% to 9.83±0.72%. This group serves as the baseline for evaluating the DNA-protective efficacy of other treatments. This group was characterized by a balanced distribution across all levels of DNA damage, confirming the intentional induction of DNA damage. Only 25.58±1.05% of cells were categorized as having normal DNA, serving as a contrasting standard to gauge the efficacy of the treatment groups. The GEE group displayed an intermediate level of DNA protection, with 53.46±2.18 of the cells categorized as Normal. This is significantly better than the positive control group but falls short when compared to the negative control. The DNA damage levels were moderate but exhibited a significant reduction compared to the Positive Control. The GEE-CNPs group showed 52.62 ± 1.97% of cells in the normal category, which is comparable to the GEE group. Despite the encapsulation of GEE in CNPs, the protective effect against DNA damage was not significantly enhanced, as evidenced by a slightly higher level of medium DNA damage. Remarkably, the CNPs group exhibited the highest percentage of 'Normal' cells among the treatment groups, at 62.96±2.97%. Although this group did not achieve the level of protection observed in the negative control, it outperformed both the GEE and GEE-CNPs groups in terms of DNA protection.

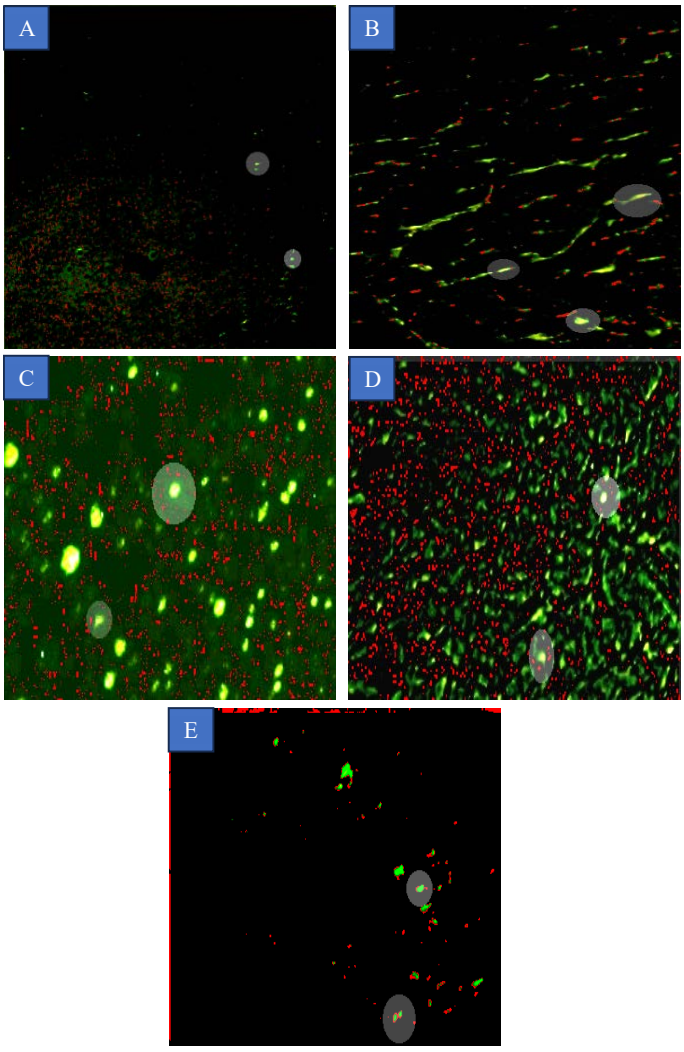

Figure 6: Images of comets of DNA damage categories in pancreatic tissue of dogs in (A) Negative contro group (non diabetic, not treated). (B) Positive control group (diabetic, saline treated) induced by alloxan–nicotinamide. (C) Ginger ethanolic extract (EE) group (diabetic, treated with 81.7 mg/kg BW GEE for 6 weeks). (D) GEE-chitosan nanoparticles (GEE-CNPs) group (diabetic,

treated with 81.7 mg/kg BW GEE-CNPs) for 6 weeks) group. (E) CNPs group (diabetic, treated with 81.7 mg/kg BW CNPs).

The CNPs group demonstrated the best DNA-protective effects among the treatment groups, followed closely by the GEE and GEE-CNPs groups. The Positive Control served its purpose in establishing a standard for DNA damage, while the Negative Control confirmed the minimal level of DNA damage expected under normal condition.

The primary objective of this study was to investigate the effects of GEE, CNPs, and GEE-CNPs on pancreatic DNA damage and histological changes in a canine model of T2D induced by Ax-Nm. The results showed significant protective effects, particularly in the groups treated with GEE-CNPs, aligning with existing literature on the pharmacological properties of ginger and chitosan.

Physicochemical characterization of nanoparticles is essential due to its influence on their cellular uptake and internalization (Shin et al., 2015). The FTIR analysis serves as a pivotal characterization technique for elucidating the chemical composition and intermolecular interactions within our nanocomposites. FTIR spectra provided substantial insights into the structural and functional integrity of GEE, CNPs, and the composite GEE-CNPs. The presence of characteristic functional groups such as OH, NH, CH, C=O, C-O, and C-N groups in the spectrum of CNPs is consistent with established literature (Abo Mansour et al., 2021; Kahdestani et al., 2021). These functional groups are not merely spectral signatures; they indicate the potential for chitosan to engage in a multitude of interactions, including hydrogen bonding and ionic interactions, thereby affecting its potential for use in drug delivery systems (Kahdestani et al., 2021). The FTIR spectrum of the GEE was equally revealing, indicating the presence of hydroxyl, alkane, carbonyl, and ether functional groups. The various compounds identified, such as aldehydes, ketones, esters, and carboxylic acids, are consistent with previous research (Zhao et al., 2015) and suggest diverse pharmacological activities that may be harnessed for therapeutic applications. The composite GEE-CNPs demonstrated a blend of functional groups from both parent materials, confirming successful loading. Additionally, the observed shifts in peak positions suggest intermolecular interactions, potentially hydrogen bonding, between chitosan and ginger extract. Such interactions could influence the stability and release kinetics of the active compounds, which is crucial for drug delivery applications (Yadav et al., 2021).

AFM provides a multi-dimensional understanding of nanoparticles, offering insights into surface topology and functional attributes that are critical for biological interactions and therapeutic applications. The amplitude parameters indicate an increase in surface roughness following GEE loading, which could be consequential for cellular uptake and bioavailability. Changes in surface skewness and kurtosis values also suggest that the nanoparticles may have improved interactions with biological systems, potentially enhancing their therapeutic efficacy. The hybrid parameters revealed significant alterations in surface curvature and slope, which could influence the nanoparticles' interaction with their biological environment. Likewise, functional parameters such as surface bearing properties and fluid retention characteristics remained relatively stable, suggesting that the encapsulation process did not negatively affect these crucial properties. One of the most noteworthy findings was the increase in summit density and surface complexity, as indicated by the spatial parameters. This increased complexity could potentially enhance the interaction of the nanoparticles with biological matrices, offering prospects for improved therapeutic outcomes.

The FTIR and AFM analyses collectively confirm the successful loading of GEE into CNPs and provide valuable insights into the potential interactions between the nanomaterials and their biological environment. These interactions could affect the stability, bioavailability, and cellular uptake of the nanoparticles, thereby influencing their therapeutic efficacy. Further studies are needed to investigate these potential effects in biological systems to validate the potential of these nanoparticles for drug delivery or other therapeutic applications.

Ginger's therapeutic properties, including its anti-diabetic effects, have been extensively studied (Zhang et al., 2021). Our findings resonate with the broader scope of research on ginger, as discussed by Unuofin et al. (2021). Their review identifies ginger as a widely used natural remedy in diabetes management, lending further support to our results on the protective effects of GEE against pancreatic DNA damage. The review complements the scientific understanding from Li et al. (2012) and Roufogalis et al. (2014), collectively reinforcing the potential of ginger-based therapies in diabetes management across different animal models, including canines.

The impact of T2D on DNA integrity is a significant area of concern that has been previously underlined in the literature. Chronic hyperglycemia and the resulting oxidative stress can induce DNA damage, thereby accelerating the aging of cells and contributing to the complications seen in T2D (Madsbad, 2016). Our study notably found that all treatment groups-GEE, CNPs, and GEE-CNPs significantly reduced DNA damage compared to the saline-treated group, as evidenced by the

comet assay results.

GEE alone demonstrated a protective effect against DNA damage. This is in line with the findings that ginger and its bioactive components, such as gingerols, exhibit anti-oxidative properties (Zhang et al., 2021). Ginger has been shown to suppress the formation of ROS, which are pivotal in the induction of DNA damage (Li et al., 2012). These anti-oxidative properties of ginger make it a potential candidate for alleviating DNA damage associated with T2D.

CNPs also exhibited a protective effect, though not as potent as the GEE-CNPs. Chitosan itself has been investigated for its anti-inflammatory and antioxidant properties (Sanjib et al., 2020). Its ability to encapsulate bioactive compounds could also contribute to its DNA-protective effects, possibly by improving the bioavailability of antioxidants.

Interestingly, the combination of GEE and CNPs, i.e., GEE-CNPs, provided the most significant protection against DNA damage. This suggests a synergistic effect between ginger's antioxidative components and chitosan's drug-delivery capabilities. Encapsulation in CNPs might have enhanced the bioavailability and stability of ginger's bioactive compounds, thereby amplifying its protective effects on DNA.

The comet assay, a sensitive method for evaluating DNA damage, supported these observations. The GEE-CNP group displayed the lowest percentage of cells with high DNA damage, substantiating the notion that nanotechnology can enhance the therapeutic efficacy of natural extracts (Nie et al., 2020).

It is worth mentioning that while our study provides valuable insights, further in-depth studies are needed to understand the mechanistic aspects of how GEE, CNPs, and GEE-CNPs exert their protective effects on DNA.

In line with the findings by Nie et al. (2020), our study also employed CNPs as a drug delivery system for GEE. Nie *et al*. highlighted the advantages of using nanoparticles in enhancing the bioavailability and efficacy of antidiabetic agents. Our results, showing a significant reduction in pancreatic DNA damage, seem to corroborate their assertions about the potential effectiveness of nanoparticle-based delivery systems in diabetes treatment.

Our results on the application of CNPs find support in the comprehensive review by Abdullaziz et al. (2022). Their work accentuates the versatility of chitosan as a bioactive material, potentially explaining the observed DNA-protective effects of chitosan in our study. Particularly, the molecular weight variants of chitosan may offer diverse benefits, a factor that warrants further investigation in future research.

The histological findings of this study corroborate the efficacy of the alloxan-nicotinamide-induced T2D model in dogs. The Positive Control group demonstrated significant pathological alterations, particularly in the islets of Langerhans and the surrounding acinar and ductal tissues, confirming the successful induction of T2D. These pathological changes are consistent with existing literature, underscoring the cytotoxic effects of alloxan and nicotinamide on pancreatic beta cells (Abdullaziz et al., 2022).

Treatment with GEE and CNPs yielded notable histological improvements. GEE treatment led to morphological normalization of the exocrine tissue and a partial restoration of the endocrine portion, as evidenced by the increased presence of Langerhans cells. These findings align with previous research highlighting the anti-inflammatory and antioxidant properties of ginger (Ayuob et al., 2021).

Intriguingly, the GEE-CNPs group displayed the most remarkable histological restoration, with significant activation and proliferation of cells in the islets of Langerhans. This suggests not only an improvement in endocrine function but also implies that the encapsulation of GEE in CNPs may offer synergistic benefits, enhancing the therapeutic efficacy of GEE. CNPs alone also showed a similar but less pronounced histological pattern, corroborating previous studies on the biocompatibility and potential therapeutic applications of chitosan nanoparticles (Nie et al., 2020).

Overall, the histological results provide valuable insights into the therapeutic efficacy of GEE and CNPs in managing T2D, particularly concerning the regeneration of islet cells. This aligns with existing studies that have discussed the potential benefits of natural compounds and nanoparticles in diabetes management (Unuofin et al., 2021). Therefore, these findings offer a promising avenue for future research into the combined application of GEE and CNPs as a treatment modality for T2D in dogs.

CONCLUSION AND RECOMMENDATIONS

This study demonstrates the successful synthesis and characterization of ginger extract-loaded chitosan nanoparticles for potential therapeutic applications in induced diabetes mellitus in dogs. The physicochemical

properties of the nanoparticles suggest that they have potential as an alternative therapy for diabetes-related complications in dogs. Further studies are required to evaluate their efficacy and safety *in vivo*. Treatment with GEE, CNPs, or GEE-CNPs protected against DNA damage and adverse histological changes in the pancreas induced by alloxan in dogs. Encapsulation of GEE in CNP improved these protective effects, highlighting the therapeutic potential of GEE-CNPs for T2D. Further investigation of GEE-CNPs as a natural antioxidant therapeutic agent for diabetic patients is justified based on these preclinical results.

ACKNOWLEDGEMENTS

N/A.

NOVELTY STATEMENT

The novelty of the study is focus on the protective effects ginger ethanolic extract loaded with chitosan nanoparticles against DNA damage and pancreatic histological changes in dogs with alloxan-nicotinamide-induced diabetes type two.

AUTHOR'S CONTRIBUTION

All authors were contributed equally.

Data availability

Data are available if requested.

Conflict of interest

The authors have declared no conflict of interest.

REFERENCES

Abba AB, Abbas DA (2019). Evaluation of lipid profile and inflammatory parameters in female diabetes type 2 induced rabbits treated with glimepride, bromocriptine and fluoxtein. Iraqi J. Vet. Med., 42(2): 97-104. https://doi.org/10.30539/iraqijvm.v42i2.305

Abdullaziz IA, Ismael MM, Metwally AM, El-Sayed MS, Elblehi SS, El-Saman AE (2022). New insights on alloxan induced canine diabetes mellitus in relation to updated therapeutic management protocols. Alex. J. Vet. Sci., 73(1): 111-1127. https://doi.org/10.5455/ajvs.108261

Abdulrazaq NB, Cho MM, Win NN, Zaman R, Rahman MT (2012). Beneficial effects of ginger (*Zingiber officinale*) on carbohydrate metabolism in streptozotocin-induced diabetic rats. Br. J. Nutr., 108(07): 1194–1201.

Abo Mansour HE, El-Batsh MM, Badawy NS, Mehanna ET, Mesbah NM, Abo-Elmatty DM (2021). Ginger extract loaded into chitosan nanoparticles enhances cytotoxicity and reduces cardiotoxicity of doxorubicin in hepatocellular carcinoma in mice. Neut. Cancer, 73(11-12): 2347-2362. https://doi.org/10.1080/01635581.2020.1823436

Akash MSH, Rehman K, Chen S (2013). Role of inflammatory mechanisms in pathogenesis of type 2 diabetes mellitus. J. Cell Biochem., 114(3): 525–531. https://doi.org/10.1002/jcb.24402

Akash MS, Rehman K, Tariq M, Chen S (2015). Zingiber officinale and Type 2 Diabetes Mellitus: Evidence from Experimental Studies. Crit Rev Eukaryot Gene Expr., 25(2): 91-112. https://doi.org/10.1615/critreveukaryotgeneexpr.2015013358

Ali MEA, Aboelfadl MMS, Selim AM, Khalil HF, Elkady GM (2018). Chitosan nanoparticles extracted from shrimp shells, application for removal of Fe (II) and Mn (II) from aqueous phases. Separat. Sci. Technol., 53(18): 2870- 2881. https://doi.org/10.1080/01496395.2018.1489845

Al-Saadi AK (2020). Nanotechnology. Research Center for Nanotechnology and Advanced Materials, University of Technology. Al Yamamah Library for Publishing and Distribution. House of Books and Documents in Baghdad 1752

Al-Salman F, Redha A, Zainab Aqeel Z, Ali Z (2022). Phytochemical content, inorganic composition, mineral profile, and evaluation of antioxidant activity of some common medicinal plants. Iraqi J. Sci., 63(7): 2764-2773. https://doi.org/10.24996/ijs.2022.63.7.1

Alshathly M (2019). Efficacy of ginger (*Zingiber officinale*) in ameliorating streptozotocin-induced diabetic liver injury in rats: Histological and biochemical studies. J. Microsc. Ultrast., 7: 91. https://doi.org/10.4103/JMAU.JMAU_16_19

Ameer DA, AL-Deen W (2023). Effect extract and nanoparticles of ginger root on pseudomonas bacteria that isolation from otitis infection. Euphrates J. Agric. Sci., 2(15): 340-350.

Anderson HR, Stitt AW, Gardiner TA, Lloyd SJ, Archer DB (1993). Induction of alloxan/streptozotocin diabetes in dogs: A revised experimental technique. Lab. Anim., 27(3): 281-285. https://doi.org/10.1258/002367793780745426

Arablou T, Aryaeian N, Valizadeh M, Sharifi F, Hosseini A, Djalali, M (2014). The effect of ginger consumption on glycemic status, lipid profile and some inflammatory markers in patients with type 2 diabetes mellitus. International Journal of Food Sciences and Nutrition, 65(4), 515-520. https://doi.org/10.3109/09637486.2014.880671

Areej B Abbas, Abbas DA (2019). Evaluation of Lipid Profile and Inflammatory Parameters in Female Diabetes Type 2 Induced Rabbits Treated with Glimepride, Bromocriptine and Fluoxtein. Iraqi J. Vet. Med., 42(2): 97–104. https://doi.org/10.30539/iraqijvm.v42i2.305

Ayuob N, Al-Shathly MR, Bakhshwin A, Al-Abbas NS, Shaer NA, Al Jaouni S, Hamed WH (2021). Rather than -catenin mediated the combined hypoglycemic effect of *Cinnamomum cassia* (L.) and zingiber officinale roscoe in the streptozotocin-induced diabetic model. Front. Pharmacol., 12: 664248. https://doi.org/10.3389/fphar.2021.664248

Behrend E, Holford A, Lathan P, Rucinsky R, Schulman R (2022). Diabetes management guidelines for dogs and cats. J. Anim. Hosp. Assoc., 54: 1–19. https://doi.org/10.5326/JAAHA-MS-6822

Bruyette D (2013). The pancreas. The Merck veterinary manual. 8th ed. Merck Sharp & Dohme Corp., USA, pp. 44-89.

Bukowiecka-Matusiak, M., Turek, I.A., Woźniak, L.A., 2014. Natural phenolic antioxidants and their synthetic derivatives. In: Systems Biology of Free Radicals and Antioxidants.

Springer: Berlin/Heidelberg, pp. 4047–4061. https://doi.org/10.1007/978-3-642-30018-9_165

Chang CLT, Lin Y, Bartolome AP, Chen YC, Chiu SC, Yang WC (2013). Herbal therapies for type 2 diabetes mellitus: Chemistry, biology, and potential application of selected plants and compounds. Evid. Based Complement. Altern. Med., 378657. https://doi.org/10.1155/2013/378657

Collins AR, Oscoz AA, Brunborg G, Gaivão I, Giovannelli L, Kruszewski M Smith, C. C., Stetina, R (2008). The comet assay: Topical issues. Mutagenesis., 23(3): 143–151. https://doi.org/10.1093/mutage/gem051

Davison L (2018). Diabetes mellitus in dogs. In Practice, 40(3): 82–92. https://doi.org/10.1136/inp.k1399

Denyer AL, Catchpole B, Davison LJ (2021). Genetics of canine diabetes mellitus part 1: Phenotypes of disease. Vet. J., 270: 105611. https://doi.org/10.1016/j.tvjl.2021.105611

Ettinger SJ, Feldman EC, Côté E (2017). Canine diabetes mellitus. In: Textbook of Veterinary Internal Medicine. SJ Ettinger and EC Feldman (eds). 8th edition. Elsevier, St Louis, Missouri., pp. 1767-1781.

Garza-Cadena C, Ortega-Rivera D M, Machorro-García G, Gonzalez-Zermeño EM, Homma-Dueñas D, Plata-Gryl M, Castro-Muñoz R (2023). A comprehensive review on Ginger (*Zingiber officinale*) as a potential source of nutraceuticals for food formulations: Towards the polishing of gingerol and other present biomolecules. Food Chem., pp. 413. https://doi.org/10.1016/j.foodchem.2023.135629

Gilor C, Niessen SJ, Furrow E, DiBartola SP (2016). What's in a name? Classification of diabetes mellitus in veterinary medicine and why it matters. J. Vet. Intern. Med., 30(4): 927–940. https://doi.org/10.1111/jvim.14357

Ibrahim HM, El-Bisi MK, Taha GM, El-Alfy EA (2015). Chitosan nanoparticles loaded antibiotics as drug delivery biomaterial. J. Appl. Pharma. Sci., 5(10): 85-90. https://doi.org/10.7324/JAPS.2015.501015

Jabar JG (2020). Preparation, characterization and analytical application of nano chitosan. Master thesis. Chemistry Dep. C. of Science Uni. of Al- Qadisiyah, pp. 33-67.

Jasim RAF (2021). Medical, pharmaceutical, and biomedical applications of chitosan: A review. Med. J. Babylon, 18(4): 291-294.

Kahdestani SA, Shahriari MH, Abdouss M (2021). Synthesis and characterization of chitosan nanoparticles containing teicoplanin using sol–gel. Polym. Bull., 78: 1133–1148 (2021). https://doi.org/10.1007/s00289-020-03134-2

Li Y, Tran VH, Duke CC, Roufogalis BD (2012). Gingerols of Zingiber officinale enhance glucose uptake by increasing cell surface GLUT4 in cultured L6 myotubes. Planta Med., 78(14): 1549-1555. https://doi.org/10.1055/s-0032-1315041

Madsbad S (2016). Impact of postprandial glucose control on diabetes-related complications: How is the evidence evolving? J. Diabetes Compl., 30: 374–385. https://doi.org/10.1016/j.jdiacomp.2015.09.019

Mahmood FA, Alwan MJ (2015). Isolation and identification of cryptococcus neoformansfrom human skin lesions and application of animal experiment (*in vivo*). Iraqi J. Vet. Med., 39(1): 85-89. https://doi.org/10.30539/iraqijvm.v39i1.202

Mahmood FA, Alwan MJ (2019). Immunopathological study of the fungus cryptococcus neoformans in mice. Iraqi J. Vet. Med., 43(1): 156–164. https://doi.org/10.30539/iraqijvm.v43i1.486

Majeed R, Mahmood AK (2023). Phytochemical and antioxidant analysis of ginger (*Zingiber officinale*) Extract loaded chitosan nanoparticles: Characterization and physicochemical properties. Adv. Anim. Sci., (*In press*).

Mohammed MA, Syeda JT, Wasan KM, Wasan EK (2017). An overview of chitosan nanoparticles and its application in non-parenteral drug delivery. Pharmaceutics, 9(4): 53. https://doi.org/10.3390/pharmaceutics9040053

Munhoz ACM, Frode TS (2018). Isolated compounds from natural products with potential antidiabetic activity. A systematic review. Curr. Diabetes Rev., 14(1): 36–106. https://doi.org/10.2174/1573399813666170505120621

Mustafa SM (2023). Herbs and plants in prophetic and modern medicine. Islamic Sci. J., 14(6): 165-189.

Nelson R, Reusch C (2014). Animal models of disease: Classification and etiology of diabetes in dogs and cats. J. Endocrinol., 222(3): T1-T9. https://doi.org/10.1530/JOE-14-0202

Nie X, Chen Z, Pang L, Wang L, Jiang H, Chen Y, Zhang Z, Fu C, Ren B, Zhang J (2020). Oral nano drug delivery systems for the treatment of type 2 diabetes mellitus: An available administration strategy for antidiabetic phytocompounds. Int. J. Nanomed., 15: 10215–10240. https://doi.org/10.2147/IJN.S285134

Niessen SJ, Bjornvad C, Church DB, Davison L, Esteban-Saltiveri D, Fleeman LM, Forcada Y, Fracassi F, Gilor C, Hanson J, Herrtage M. (2022). Agreeing language in veterinary endocrinology (ALIVE): Diabetes mellitus-a modified Delphi-method-based system to create consensus disease definitions. Vet. J., 289: 105910. https://doi.org/10.1016/j.tvjl.2022.105910

Nikolić M, Vasić S, Đurđević J, Stefanović O, Čomić L (2014). Antibacterial and anti-biofilm activity of ginger (*Zingiber officinale* (Roscoe)) ethanolic extract. Kragujevac J. Soc., 36: 129-136. https://doi.org/10.5937/KgJSci1436129N

O'Kell AL, Davison LJ (2023). Etiology and pathophysiology of diabetes mellitus in dogs. The Veterinary clinics of North America. Small Anim. Pract., 53(3): 493–510. https://doi.org/10.1016/j.cvsm.2023.01.004

O'Kell AL, Wasserfall C, Catchpole B, Davison LJ, Hess RS, Kushner JA, Atkinson MA (2017). Comparative pathogenesis of autoimmune diabetes in humans, NOD mice, and canines: Has a valuable animal model of type 1 diabetes been overlooked? Diabetes, 66(6): 1443–1452. https://doi.org/10.2337/db16-1551

Papachristoforou E, Lambadiari V, Maratou E, Makrilakis K (2020). Association of glycemic indices (hyperglycemia, glucose variability, and hypoglycemia) with oxidative stress and diabetic complications. J. Diabetes Res., pp. 7489795. https://doi.org/10.1155/2020/7489795

Pires CT, Vilela JA, Airoldi C (2014). The effect of chitin alkaline deacetylation at different condition on particle properties. Proc. Chem., 9: 220-225. https://doi.org/10.1016/j.proche.2014.05.026

Poitout V, Robertson RP (2008). Glucolipotoxicity: Fuel excess and β-cell dysfunction. In Endocrine Reviews, 29(3): 351–366. https://doi.org/10.1210/er.2007-0023

Priyanka DN, Prashanth KH, Tharanathan, RN (2022). A review on potential anti-diabetic mechanisms of chitosan and its derivatives. Carbohydrat. Polymer Technolog. Applicat., 3: 100188. https://doi.org/10.1016/j.carpta.2022.100188

Roufogalis BD (2014). Zingiber officinale (Ginger): A Future Outlook on Its Potential in Prevention and Treatment of Diabetes and Prediabetic States. New J Sci., 2014: 674684..

http://dx.doi.org/10.1155/2014/674684

Salih SI, Al-Mutheffer EA, Mahdi AK, Al-Naimi RAS (2015). Role of chitosan application in postoperative abdominal adhesions in rabbits. Iraqi J. Vet. Med., 39(1): 105–111. https://doi.org/10.30539/iraqijvm.v39i1.206

Sanjib S, Dibyendu D, Prachurjya D, Jatin K, Sawlang BW, Prasenjit, M (2020). Chitosan: A promising therapeutic agent and effective drug delivery system in managing diabetes mellitus. Carbohydrate Polymers, 247: 116594. https://doi.org/10.1016/j.carbpol.2020.116594

Sari D R, Ahmad FF, Djabir YY, Yulianty R (2020). Breadfruit leaves extract (*Artocarpus altilis*) effect on pancreatic damage in diabetic type II animal model induced by alloxan–nicotinamide. Med. Clín. Práct., 3(1): 100099. https://doi.org/10.1016/j.mcpsp.2020.100099

Shin SW, Song IH, Um SH (2015). Role of physicochemical properties in nanoparticle toxicity. Nanomaterials (Basel), 5(3): 1351–1365. https://doi.org/10.3390/nano5031351

Singh NP, McCoy MT, Tice RR, Schneider EL (1988). A simple technique for quantitation of low levels of DNA damage in individual cells. Exp. Cell Res., 175(1): 184-191. https://doi.org/10.1016/0014-4827(88)90265-0

SPSS Inc. (2007). SPSS for Windows, Version 16.0. Chicago, SPSS Inc.

Suvarna KS, Layton C, Bancroft JD (2018). Bancroft's theory and practice of histological techniques. Elsevier Health Sci., 5(7): 23-45.

Uchigata Y, Yamamoto H, Nagai H, Okamoto H (1983). Effect of poly (ADP-ribose) synthetase inhibitor administration to rats before and after injection of alloxan and streptozotocin on islet proinsulin synthesis. Diabetes, 32(4): 316-318. https://doi.org/10.2337/diab.32.4.316

Unuofin JO, Masuku NP, Paimo OK, Lebelo SL (2021). Ginger from farmyard to town: Nutritional and pharmacological applications. Front. Pharmacol., 12: 779352. https://doi.org/10.3389/fphar.2021.779352

Vattam KK, Raghavendran H, Murali MR, Savatey H, Kamarul T (2016). Coadministration of alloxan and nicotinamide in rats produces biochemical changes in blood and pathological alterations comparable to the changes in type II diabetes mellitus. Hum. Expert. Toxicol., 35(8): 893-901. https://doi.org/10.1177/0960327115608246

Yadav P, Yadav AB (2021). Preparation and characterization of BSA as a model protein loaded chitosan nanoparticles for the development of protein-/peptide-based drug delivery system. Futur. J. Pharm. Sci., 7: 200. https://doi.org/10.1186/s43094-021-00345-w

Zhang M, Zhao R, Wang D, Wang L, Zhang Q, Wei S, Lu F, Peng W, Wu (2021). Ginger (*Zingiber officinale* Rosc.) and its bioactive components are potential resources for health beneficial agents. Photother. Res., 35(2): 711-742. https://doi.org/10.1002/ptr.6858

Zhao X, Zhu H, Chen J, Ao Q (2015). FTIR, XRD and SEM analysis of ginger powders with different size. J. Food Process. Preservat., 39(6): 2017-2026. https://doi.org/10.1111/jfpp.12442